Geophysical Research Letters

RESEARCH LETTER

10.1029/2020GL090281

Key Points:

- Underwater glider observations are used to produce three-dimensional estimates of mean and eddy kinetic energy in and near the Gulf Stream
- Mean and eddy kinetic energy generally decay exponentially with depth and have somewhat longer decay scales within the Gulf Stream
- Three-dimensional mean and eddy kinetic energy fields are available for further analyses and will be updated with future observations

Supporting Information:

- Supporting Information S1

Correspondence to:

R. E. Todd,
rtodd@whoi.edu

Citation:

Todd, R. E. (2021). Gulf Stream mean and eddy kinetic energy: Three-dimensional estimates from underwater glider observations. *Geophysical Research Letters*, *48*, e2020GL090281. https://doi.org/10.1029/2020GL090281

Received 18 AUG 2020
Accepted 22 JAN 2021

Gulf Stream Mean and Eddy Kinetic Energy: Three-Dimensional Estimates From Underwater Glider Observations

Robert E. Todd[1]

[1]Physical Oceanography Department, Woods Hole Oceanographic Institution, Woods Hole, MA, USA

Abstract The strong, meandering, and eddy-shedding Gulf Stream is a large oceanic reservoir of both mean and eddy kinetic energy in the northwestern Atlantic. Since 2015, underwater gliders equipped with Doppler current profilers have collected over 20,000 absolute velocity profiles in and near the Gulf Stream along the US East Coast. Those observations are used to make three-dimensional estimates of mean and eddy kinetic energy, substantially expanding the geographic coverage of prior estimates of subsurface kinetic energy in the Gulf Stream. Glider observations are combined via weighted least squares fitting with anisotropic and inhomogeneous length scales to reflect both circulation and sampling density; this averaging technique can be applied to other quantities measured by the gliders. Mean and eddy kinetic energy decay approximately exponentially away from the surface. Vertical decay scales are longest within the high-speed core of the Gulf Stream and somewhat shorter on the flanks of the Gulf Stream.

Plain Language Summary Energy is a key metric of the Earth's climate system, of which the ocean is a major part. Kinetic energy, the energy of moving water in the ocean, is partitioned into mean kinetic energy that is associated with the time-averaged ocean circulation and eddy kinetic energy that is associated with time-varying motions. Here, a large set of velocity measurements collected by autonomous underwater gliders is used to make three-dimensional estimates of mean and eddy kinetic energy in and near the Gulf Stream, one of the strongest currents in the global ocean. These new estimates of oceanic kinetic energy serve as a benchmark for numerical simulations of the ocean and climate system to reproduce.

1. Introduction

Energy budgets of the ocean-atmosphere system are key to understanding the functioning of the Earth's climate system. The ocean is a major reservoir of both kinetic energy (see Ferrari & Wunsch, 2009, and references therein) and potential energy (Roullet et al., 2014). Subtropical western boundary currents, with their high velocities and tendency to meander and shed large eddies, are regions of high mean kinetic energy (MKE) and eddy kinetic energy (EKE) (e.g., Wyrtki et al., 1976; Yu et al., 2019); the same regions also serve as sinks of eddy energy due to westward propagation of eddies toward the boundaries (Zhai et al., 2010). The Gulf Stream is the subtropical western boundary current of the North Atlantic, flowing along the US East Coast with characteristic speeds near 1 m s^{-1} (Heiderich & Todd, 2020). Near Cape Hatteras, NC (~35.5°N), the Gulf Stream separates from the continental margin, after which its meanders grow (e.g., Watts & Johns, 1982, and references therein) and it sheds large eddies (e.g., Richardson, 1983). Both instabilities of the flow and topographic effects where the Gulf Stream flows along the continental margin lead to spatially varying transfers of kinetic energy between the mean and time-varying flows (e.g., Dewar & Bane, 1985; Gula et al., 2015, 2016; Kang & Curchitser, 2015; Rossby, 1987; Todd, 2017).

Estimates of oceanic kinetic energy require observations of ocean velocity, which is less commonly measured than hydrographic properties (Szuts et al., 2019). Observation-based estimates of kinetic energy are particularly sparse within the ocean interior, which is not sampled by satellites (Cole et al., 2020). For the Gulf Stream region, various estimates of the surface kinetic energy have been made from surface drifter and satellite altimetry measurements (e.g., Richardson, 1983a; Rypina et al., 2012), and similar global estimates are available (e.g., Stammer, 1997; Wyrtki et al., 1976; Yu et al., 2019). Subsurface estimates of kinetic energy in the Gulf Stream, and elsewhere in the ocean, are less common and have typically been limited to two spatial dimensions and/or small regions. Richardson (1983c) combined observations from drifting buoys, acoustically tracked floats, and moored current meters (e.g., Schmitz, 1978) to produce the first section of EKE across the Gulf Stream at 55°W. Subsequent analyses of observations along repeatedly sampled transects have yielded additional cross-stream sections of EKE (e.g., Halkin & Rossby, 1985; Rossby & Gottlieb, 1998; Rossby, 1987). Horizontal distributions of EKE at select depths have been produced using arrays of moored current meters (Schmitz, 1976, 1984; Shay et al., 1995) and acoustically tracked floats (Owens, 1991).

Here, we use multiyear observations collected by autonomous underwater gliders to produce three-dimensional estimates of kinetic energy in the upper 1,000 m for the Gulf Stream region along the US East Coast, building on the existing set of two-dimensional estimates for the region. The observations and the methodology developed for analyzing them are presented in Section 2 with further details and estimates of errors arising from measurement uncertainty provided in the online supporting information. In Section 3, glider-based kinetic energy estimates are shown to compare favorably to satellite-based estimates and then are used to examine the lateral and vertical distributions of MKE and EKE in and near the Gulf Stream along the US East Coast. Section 4 briefly summarizes the results and implications.

2. Observations and Methods

2.1. Spray Glider Observations

Spray gliders (Rudnick et al., 2016; Sherman et al., 2001) have collected absolute velocity profiles in and near the Gulf Stream since July 2015 (Heiderich & Todd, 2020; Todd, 2017) using 1-MHz Nortek AD2CP Doppler current profilers (Todd et al., 2017). Over the course of 31 missions completed through June 2020, gliders have returned 20,525 absolute velocity profiles in and near the Gulf Stream between Miami, FL (~25.8°N) and Cape Cod, MA (~41°N; Figure 1a). The density of observations is highest near Cape Hatteras, NC (~36°N along 74.7°W) where a 2-year sampling campaign for the "Processes driving Exchange At Cape Hatteras" program (PEACH; Todd, 2020a) took place in parallel with longer-term Gulf Stream sampling. Sampling density is lowest downstream (northeast) of Cape Hatteras due to several shark attacks and various instrument failures cutting glider missions short.

Individual velocity profiles typically extend to within a few meters of the seafloor or to a maximum depth of 1,000 m with 10-m resolution and have a typical accuracy of 0.1 m s^{-1} (Heiderich & Todd, 2020). PEACH glider missions most often sampled to a maximum depth of 500 m (Todd, 2020a), and some gliders sampling in or near the Gulf Stream were restricted to shallower dives due to problems arising late in their missions. Velocity profiles from two missions are noisier due to the loss of raw data for postprocessing (see Heiderich & Todd, 2020); those profiles are used only for computations of mean velocity in the following analysis.

2.2. Satellite Altimetry

Estimates of absolute dynamic topography (ADT) and surface geostrophic velocity on a 0.25° × 0.25° grid were obtained from the European Union (EU) Copernicus Marine Environment Monitoring Service (CMEMS) multimission satellite altimetry products. To approximately match the temporal coverage of the glider observations while using an integral number of years of data, we use altimetry products for the period July 1, 2015 through June 30, 2020. Delayed-mode data are used up to October 15, 2019 with near-real time data for the balance of the period. Following Heiderich and Todd (2020), we use the time-average position of the 40-cm ADT contour to define an along-stream coordinate that, as shown below, follows the mean path of the Gulf Stream. Distance along this contour is measured from 25°N, and we define cross-stream transects I–IV at along-stream distances of 500, 1,000, 1,300, and 1,700 km for further examination (Figure 1a).

2.3. Averaging Algorithm and Estimating Kinetic Energy

For an appropriate averaging operation $\langle\cdot\rangle$, the horizontal velocity is divided into mean and fluctuating parts as $(u,v) = \left(\langle u\rangle,\langle v\rangle\right) + (u',v')$. The mean and eddy kinetic energy are then defined as

$$\mathrm{MKE} = \frac{1}{2}\left(\langle u\rangle^2 + \langle v\rangle^2\right) \quad (1)$$

10.1029/2020GL090281

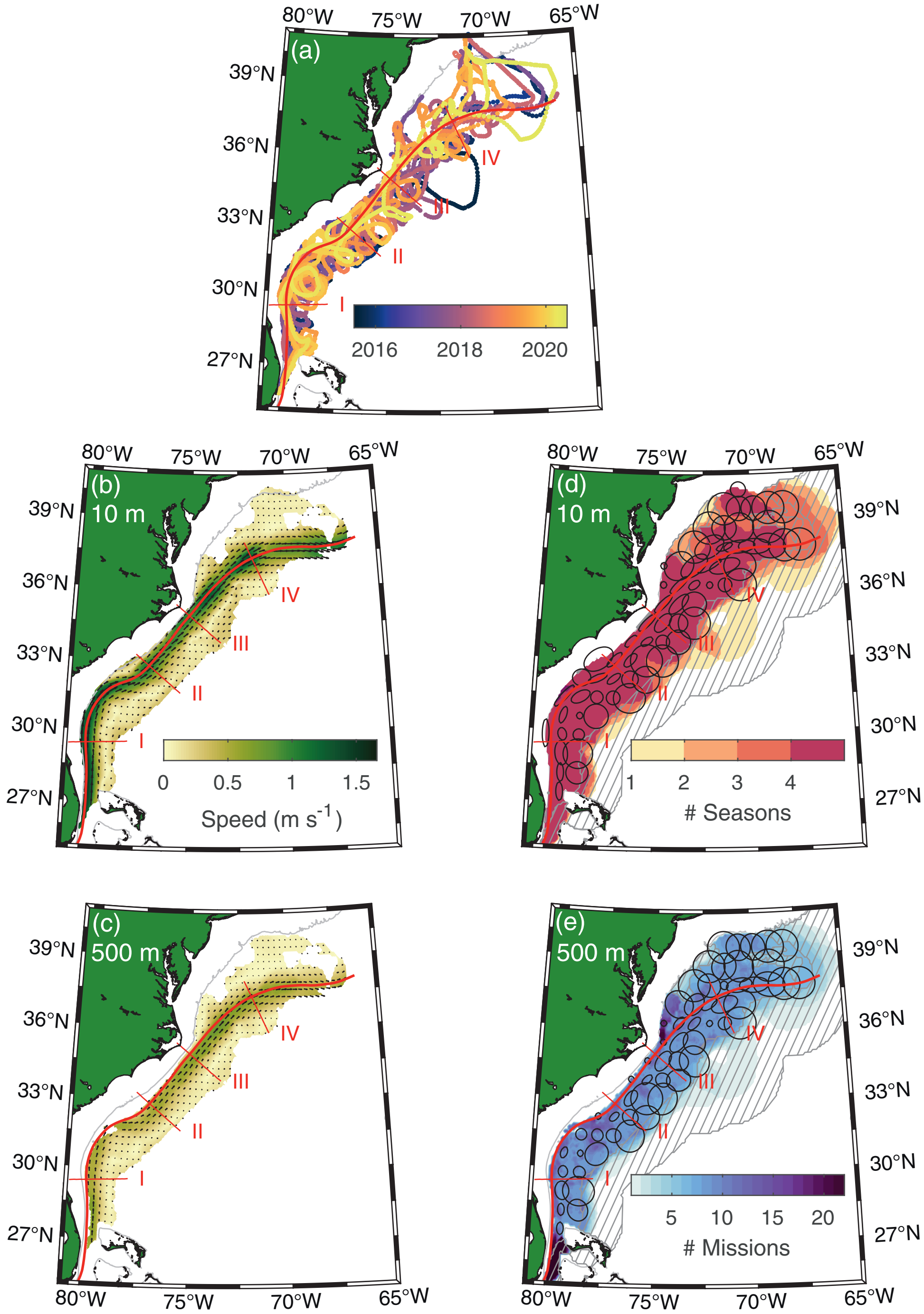

Figure 1. (a) Spray glider sampling in and near the Gulf Stream during July 2015–June 2020. (b and c) Mean currents at depths of (b) 10 m and (c) 500 m with vectors plotted at every third grid point for clarity. (d) Number of seasons with data at 10 m weighted greater than exp (−1); ellipses, which are shown at every fifth grid point for clarity, denote the scales L_1 and L_2 and mean flow direction α as well the region over which the weight function exceeds exp (−1) at those grid points. (e) As in (d), but for number of missions with data at 500 m weighted greater than exp (−1). Hatched regions in (d–e) show where mean values in (b–c) and elsewhere are masked due to inadequate sampling as described in the text. In all panels, the bold red line is the mean location of the 40-cm ADT contour; thin red lines are cross-stream transects I–IV that are examined below. ADT, absolute dynamic topography.

10.1029/2020GL090281

$$\mathrm{EKE} = \frac{1}{2}\left\langle u'^2 + v'^2 \right\rangle. \tag{2}$$

The choice of the averaging operation is critical as it determines the meaning of "eddy."

To estimate MKE and EKE from glider observations, we choose to compute a two-dimensional, Gaussian-weighted planar fit on a 0.1° × 0.1° grid at each depth using a weighted least squares approach. Details of the least squares procedure are included in the online supporting information. The Gaussian weight function at a given grid point and depth is defined as

$$W(r,s) = \exp\left(-\frac{r^2}{L_1^2} - \frac{s^2}{L_2^2}\right), \tag{3}$$

where r is the along-mean-flow distance from the grid point, s is the cross-mean-flow distance from the grid point, and L_1 and L_2 are the corresponding e-folding scales. We interpret the fit as an Eulerian time average at each location. A planar fit is used instead of a Gaussian weighted mean to better match observations in the presence of the strong gradients associated with the Gulf Stream and to avoid bias when observations are not uniformly distributed around a grid point (e.g., near Cape Hatteras due to dense PEACH sampling). We use a Gaussian weight function that is anisotropic and inhomogeneous to account for both expected differences in spatial scales in the presence of a strong mean flow (i.e., the Gulf Stream) and the varying density of observations (Figure 1a). Similar averaging operations have been applied to other sets of observations (Owens, 1991; Ridgway et al., 2002; Roemmich & Gilson, 2009).

The finite speed of the gliders sets a lower limit on the spatial scales that can be resolved due to the mixing of spatial and temporal variability (Rudnick & Cole, 2011). Frequency spectra of glider-based velocity estimates (not shown) exhibit a change in slope near a frequency $f_0 = 0.03$ cycles per hour (cph), consistent with other analyses of Spray glider observations (Rudnick & Cole, 2011; Rudnick et al., 2017; Todd, 2020a), suggesting an upper limit for resolved frequencies and wavenumbers (Rudnick et al., 2017). For a glider moving at a typical horizontal speed of $u_g = 0.25$ m s^{-1} in still water, the equivalent along-track wavenumber is $\kappa_0 = f_0/u_g = 0.03$ cycles per kilometer (cpkm). The Fourier transform $\widehat{W}(k,l)$ of the Gaussian weight function (3) is the similar Gaussian

$$\widehat{W}(k,l) = L_1 L_2 \pi \exp\left(-\pi^2 (k^2 L_1^2 + l^2 L_2^2)\right), \tag{4}$$

where k and l are along- and cross-flow components of the horizontal wavenumber, respectively. Following Rudnick et al. (2017), a homogeneous length scale of 15 km would result in the exponential in Equation 4 having an argument of −2 at wavenumbers with magnitudes $\sqrt{k^2 + l^2} = \kappa_0$.

Since gliders are advected downstream while steering perpendicular to measured currents within the Gulf Stream, we modify the relationship between the maximum resolved along-flow wavenumber κ_0 and frequency f_0 to be

$$k_0 = \frac{f_0}{\max(u_g, u_w)}, \tag{5}$$

where u_w is the local mean current speed. The corresponding minimum value of L_1 that makes the argument of Equation 4 equal to −2 at $(k, l) = (k_0, 0)$ is

$$L_{1,\min} = \frac{\sqrt{2}}{\pi k_0}. \tag{6}$$

For currents faster than the glider's speed, the maximum resolved along-flow wavenumber shrinks and the minimum resolved along-flow spatial scale increases. At a typical Gulf Stream speed of 1 m s^{-1}, $L_{1,\min} = 54$ km. In the cross-flow direction, the relationship between maximum resolved wavenumber l_0 and

10.1029/2020GL090281

frequency is simply $l_0 = f_0/u_g$, since the mean cross-flow current is zero by construction, and $L_{2,\min} = 15$ km results in the argument of Equation 4 being -2 at $(k, l) = (0, l_0)$.

We determine the final scales L_1 and L_2 and the direction of flow α at each grid point as follows. As a first guess, we take $L_1 = L_2 = 15$ km (the minimum values in still water) and evaluate the weight function (3) for each velocity estimate at a depth of 10 m (our shallowest level). To avoid large sampling bias, if observations weighted greater than exp (-1) do not come from at least eight glider missions, all four seasons (defined as January–March, April–May, etc.), and do not span at least 180° about the grid point, then the scales L_1 and L_2 are iteratively increased by 10% up to a maximum of 75 km. Setting weights to zero where $W(r, s) < 0.001$ for computational efficiency, we then make a first estimate of mean velocity at that depth. The magnitude of the resulting velocity gives an updated $L_{1,\min}$ using Equations 5–6, and the direction of the mean current defines the along-flow direction α, both of which are used with $L_2 = 15$ km to update the weight function. Scales are again incrementally increased up to a maximum of 75 km (allowing L_1 to exceed 75 km for strong currents) to ensure adequate sampling, and then the estimate of velocity is updated. This cycle repeats until the magnitude of the velocity change is less than 1% of the mean velocity estimate. Parameters defining the weight function (3) for successively deeper levels are produced similarly, but with scales from the next shallowest depth used as the initial guess for computational efficiency.

The weight function (3) and three-dimensional fields of L_1, L_2, and α define our averaging function ($\langle\cdot\rangle$ in Equations 1 and 2) for glider-based observations in the vicinity of the Gulf Stream. The weight function is localized in space, but unrestricted in time, justifying our interpretation of resulting fields as time averages over the 5-year period of the glider observations with defined spatial resolution. The mean velocity field (e.g., Figure 1b and 1c) captures the swift, narrow Gulf Stream with stronger velocities at the surface (Figure 1b) than at depth (Figure 1c). Throughout the domain, the strongest flows are well-aligned with the time-mean 40-cm ADT contour (Figure 1b), which serves as an independent estimate of Gulf Stream path (Heiderich & Todd, 2020; Todd et al., 2016). Both glider-based mean velocity and the 40-cm ADT contour capture local features like the offshore deflection near 32°N that results from the Gulf Stream impinging upon the topographic barrier of the Charleston Bump (Bane & Dewar, 1988; Gula et al., 2015; Legeckis, 1979). Dense sampling along the axis of the Gulf Steam (Figure 1a) allows for small values of L_2 (e.g., Figure 1d and 1e), so that the mean captures the sharp cross-stream gradients within the Gulf Stream while allowing for larger along-stream scales where advection is strongest. On the margins of the Gulf Stream, less dense sampling and weak mean currents result in larger and more isotropic scales (e.g., Figure 1d and 1e). Errors in $\langle u\rangle$ and $\langle v\rangle$ due to random errors in individual velocity profiles are typically less than 0.02 m s^{-1} (see Figure S1b).

We estimate MKE and EKE from glider-based velocity measurements using 1 and 2 with $\langle\cdot\rangle$ representing the averaging algorithm described above. Errors in the MKE and EKE estimates due to random errors in individual velocity profiles are generally less than 10% of the MKE or EKE, except where MKE is near zero (see Figure S2). We note that three-dimensional mean fields of other quantities measured by the gliders may be computed using the same averaging algorithm. We mask estimates of averaged quantities where the number of seasons or number of missions with data weighted greater than exp (-1) is less than three or six, respectively (e.g., Figure 1d and 1e); as shown in the online supporting information, this masking effectively removes estimates with large errors due to errors in the underlying measurements.

3. Results

3.1. Comparison With Satellite-Based Estimates

To assess the robustness of our glider-based estimates of MKE and EKE, we first compare our estimates at a depth of 10 m to independent estimates of MKE and EKE from satellite-based surface geostrophic velocity estimates (Figure 2). Satellite-based estimates are simply computed using Eulerian time averages at each 0.25° × 0.25° grid point, but noting that the gridded altimetry product is limited to resolving features with wavelengths longer than about 200 km or feature scales larger than about 50 km (Chelton et al., 2011, 2019).

Estimates from both sets of observations give broadly similar distributions of MKE (Figures 2a and 2b) with maximum values along the Gulf Stream axis of 0.5–1.3 m^{2}s^{-2} (corresponding to mean near-surface speeds of 1.0–1.6 m s^{-1}; Figure 2i). Comparisons of MKE estimates along select cross-Gulf Stream transects

10.1029/2020GL090281

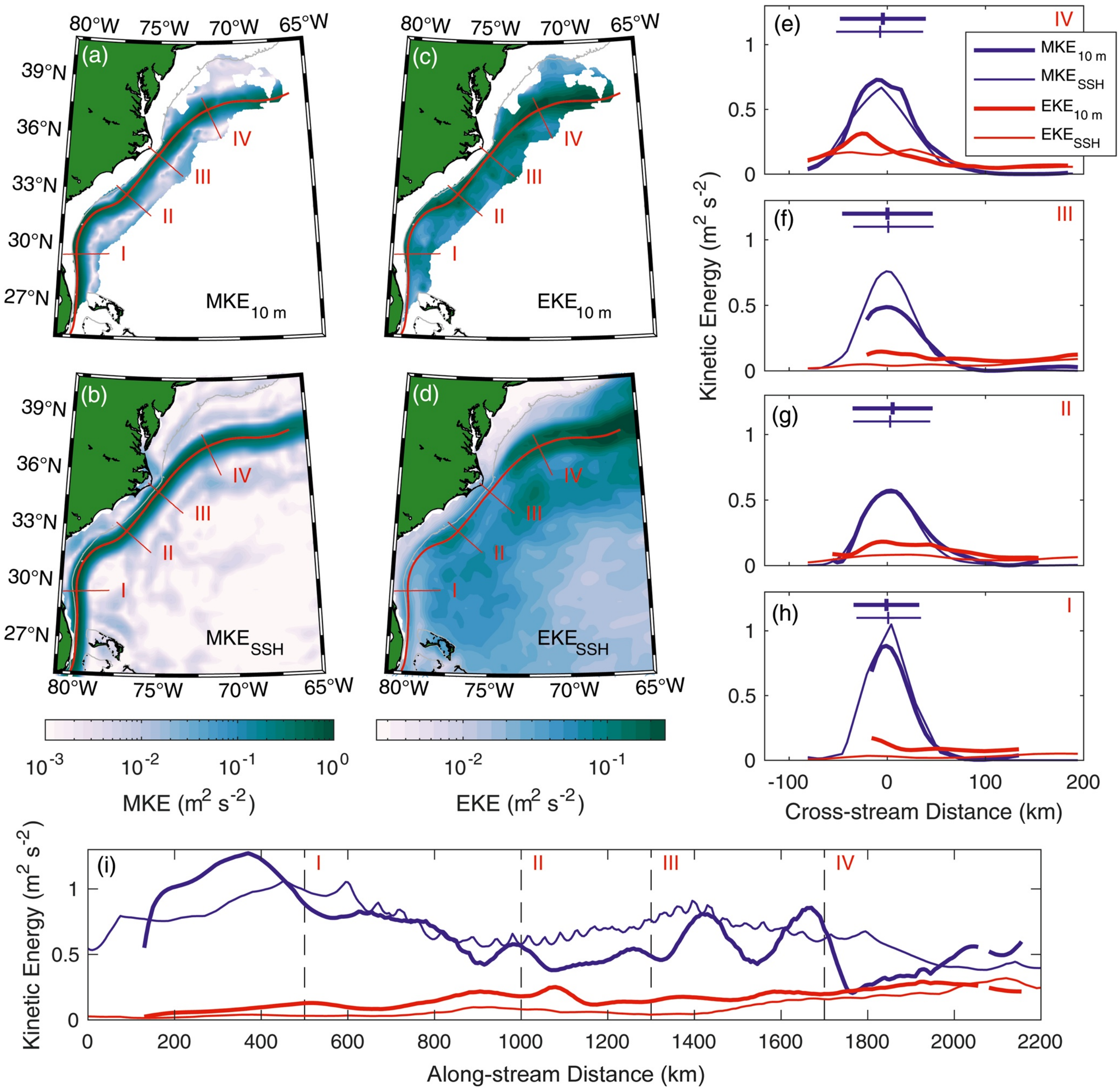

Figure 2. Near-surface kinetic energy estimates from gliders and satellite altimetry. (a and b) MKE (a) at a depth of 10 m from glider measurements and (b) at the surface from satellites. (c and d) EKE (c) at 10 m from glider measurements and (d) at the surface from satellites. Note that the color scale for EKE has an order of magnitude less range than that for MKE. (e–h) MKE (blue) and EKE (red) along transects I–IV (arranged bottom-to-top) with thick lines for glider-based estimates and satellite-based estimates shown thin. Blue bars at the top of each panel show the center and *e*-folding scale of a Gaussian fit to the glider- (thick) and satellite-derived (thin) MKE along each transect. (i) MKE (blue) and EKE (red) along the mean 40-cm ADT contour with glider- and satellite-based estimates shown thick and thin, respectively. ADT, absolute dynamic topography; EKE, eddy kinetic energy; MKE, mean kinetic energy.

(Figures 2e–2h) and along the axis of the Gulf Stream (Figure 2i) show that the two estimates of MKE match particularly well in the Gulf Stream as it flows along the continental margin offshore of Georgia and South Carolina (between transects I and II; Figures 2g–2i). This area has been particularly well sampled by gliders (Figure 1) and is also a region where the presence of stabilizing slope topography minimizes meander amplitude (see Gula et al., 2015), so the sampling adequately averages over the intrinsic variability. Approaching Cape Hatteras (near transect III) and at some points downstream (northeast) of Cape Hatteras, the glider-based MKE estimate is markedly lower than the satellite-based estimate (e.g., Figures 2f and 2i).

During some sampling periods, transient shifts in Gulf Stream position led to weak currents along the time-mean axis of the Gulf Stream. Since glider sampling is less dense downstream of Cape Hatteras (Figure 1) and the magnitude of lateral Gulf Stream meanders is larger, the glider-based time-mean is not yet adequately constrained, despite the extensive, multiyear sampling effort; estimates of the effective number of degrees of freedom resulting from the glider sampling are lower in this region (see Figure S1a). Within the narrow Florida Strait (south of ~27.5°N) and immediately downstream to near transect I, the glider-based MKE estimate generally exceeds the satellite-based estimate (Figure 2i, along-stream distance less than 500 km), potentially as a result of land-based interference or marginal spatial resolution in the gridded, satellite-based products. To first order, MKE has a roughly Gaussian cross-stream structure (Figures 2e–2h) in both the glider-based and satellite-based estimates, consistent with prior results (e.g., Kelly & Gille, 1990). Least squares fitting of a Gaussian to the MKE estimates at each along-stream position thus provides a way to characterize the position and width of the Gulf Stream core. Large MKE associated with the Gulf Stream core is centered within about 10 km of the mean position of the 40-cm ADT contour over the domain in Figure 2 and has a cross-stream *e*-folding scale that is ~35 km upstream of Cape Hatteras and then increases to at least 42 km by transect IV downstream of Cape Hatteras (Figures 2e–2h).

Glider-based and satellite-based EKE estimates show the same broad spatial structure, but more differences between estimation techniques are apparent than for MKE (Figure 2c and 2d). EKE is high along the core of the Gulf Stream with largest values downstream of Cape Hatteras in the open North Atlantic, where the Gulf Stream exhibits large meanders that Rossby (1987) previously showed contribute most of the observed variability. Another local maximum is apparent near the Charleston Bump (~32°N), where meander amplitude has a local maximum (Bane & Dewar, 1988; Gula et al., 2015; Legeckis, 1979; Zeng & He, 2016). Glider-based EKE estimates are usually larger than satellite-based estimates, particularly upstream (southwest) of Cape Hatteras, where the Gulf Stream flows along the continental margin (Figures 2f–2h); the gliders likely capture smaller-scale variability that is not resolved by the gridded altimetry. Away from the core of the Gulf Stream, EKE estimates from both sets of observations plateau around 0.1 m^2s^{-2} as compared to the near-zero values of MKE away from the Gulf Stream.

These comparisons between glider-based and satellite altimetry-based estimates of near-surface MKE and EKE (Figure 2), particularly along the well-sampled and weakly meandering portion of the Gulf Stream offshore of Georgia and South Carolina and in the quiescent regions away from the Gulf Stream, give confidence that our methodology for averaging the glider observations is reasonable. We neither seek nor expect perfect agreement between kinetic energy estimates from gliders and satellites owing to the differences in resolved scales and processes. Indeed, estimates of surface kinetic energy distributions from various observational and numerical products have been shown to vary markedly in magnitude while exhibiting broadly consistent spatial patterns (e.g., Cole et al., 2020). Instead, having shown reasonable consistency between the glider-based estimates of kinetic energy and an independent estimate at the surface, our primary goal is to exploit the subsurface glider observations to characterize the three-dimensional distribution of MKE and EKE in and near the Gulf Stream.

3.2. Three-Dimensional Kinetic Energy Distributions

The lateral structure of MKE and EKE apparent at the surface (Figure 2) is generally consistent through the upper kilometer of the water column, but with magnitudes decreasing with depth (Figure 3). The local maximum in MKE along the axis of the Gulf Stream shifts offshore with increasing depth (Figures 3e–3h), consistent with many previous studies of Gulf Stream velocity structure (e.g., Andres et al., 2020; Halkin & Rossby, 1985; Johns et al., 1995; Rossby & Zhang, 2001; Todd et al., 2016). Downstream of Cape Hatteras some small discontinuities are apparent in the MKE fields at depths near 350, 500, and 750 m (Figures 3e, 3f and 3i), which we attribute to differences in maximum sampling depths for some glider missions. Enhanced EKE in the vicinity of the Charleston Bump (near transect II) and downstream of Cape Hatteras (near transect IV) penetrates throughout the upper several hundred meters of the water column (Figures 3c, 3d and 3i). Averaged in the along-stream direction, the cross-stream location of the EKE maximum associated with the Gulf Stream core is typically O(10) km shoreward of the MKE maximum at the same depth. This shoreward intensification of EKE likely results from the asymmetry of the Gulf Stream, which has stronger

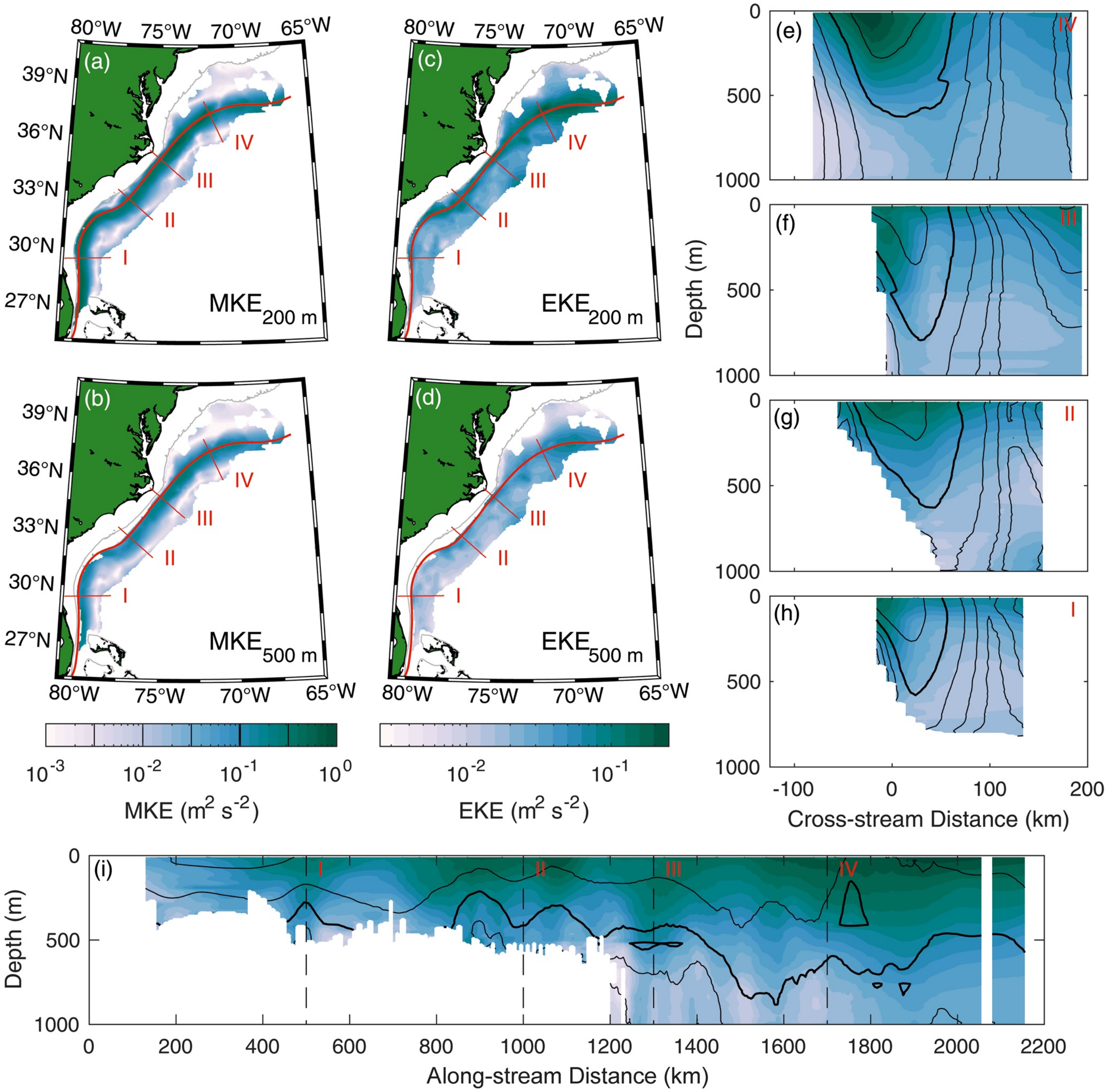

Figure 3. Examples of the three-dimensional structure of kinetic energy in and near the Gulf Stream. (a and b) Maps of MKE at depths of (a) 200 m and (b) 500 m. (c and d) As in (a and b), but for EKE. (e–h) Cross-Gulf Stream transects of EKE (colors) and MKE (black contours every $10^{0.5}$ m^{2}s^{-2} with the 10^{-1} m^{2}s^{-2} contour bold) along transects I–IV (arranged bottom-to-top). (i) EKE (color) and MKE (black contours) along the mean 40-cm ADT contour. Note that the color scale for EKE has an order of magnitude less range than that for MKE. ADT, absolute dynamic topography; EKE, eddy kinetic energy; MKE, mean kinetic energy.

lateral shear on its shoreward (western or northern) edge (e.g., Halkin & Rossby, 1985; Johns et al., 1995) so that lateral shifts in position result in larger velocity perturbations relative to the mean.

To better characterize the vertical structure of MKE and EKE, we seek appropriate vertical length scales for the observed decay with depth. We compute mean profiles of MKE and EKE for three distinct regions (Figure 4): (1) greater than 50 km inshore of the 40-cm ADT contour, (2) the core of the Gulf Stream within 50 km on either side of the 40-cm ADT contour, and (3) more than 50 km offshore of the 40-cm ADT

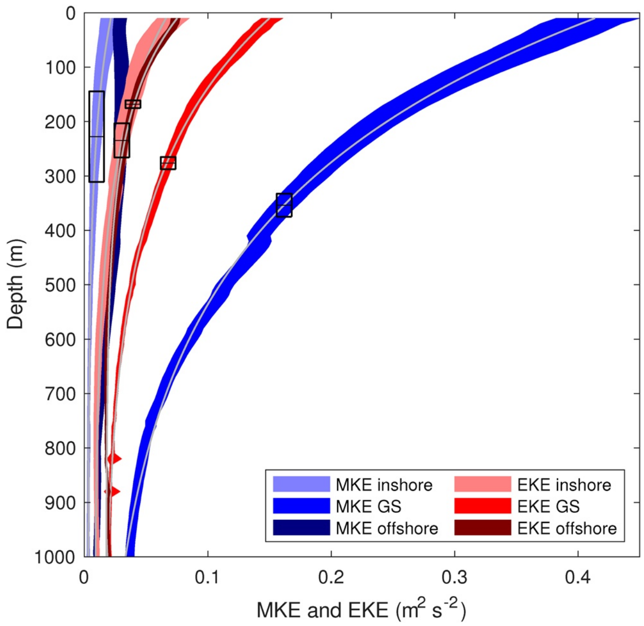

Figure 4. Mean profiles of MKE (blues) and EKE (reds) inshore of the Gulf Stream (light colors), within 50 km of the 40-cm ADT contour (medium colors), and offshore of the Gulf Stream (dark colors). Profile widths represent the mean plus or minus one standard error at each depth. Gray curves are least squares fits as described in the text with black boxes indicating the mean ± one standard deviation of the *e*-folding depths for the fits. ADT, absolute dynamic topography; EKE, eddy kinetic energy; MKE, mean kinetic energy.

contour. Standard errors of these mean profiles are constructed by estimating the number of degrees of freedom as the ratio of total area of the region of interest to the average area over which the weight function at individual grid points exceeds exp (-1) within that region. Mean profiles of MKE and EKE within the energetic core of the Gulf Stream differ from those on the flanks by many standard errors, except for EKE deeper than 850 m. At depths near 1,000 m in the core of the Gulf Stream, EKE is typically 0.01–0.03 m^2s^{-2} (Figures 3e–3g, 3i, and 4), in good agreement with values inferred by Richardson (1983c) at 55°W and Rossby (1987) at 73°W. MKE offshore of the Gulf Stream is typically larger than MKE inshore of the Gulf Stream core, whereas mean EKE profiles inshore and offshore of the Gulf Stream are similar throughout most of the observed water column. While EKE is less than MKE within the core of the Gulf Stream, it exceeds MKE at various depths, particularly shallower than 150 m, on both flanks of the Gulf Stream.

We estimate vertical decay scales of MKE and EKE via least squares fitting of an exponential plus a constant to the mean profiles in Figure 4. The constant is added since most profiles appear to plateau at a nonzero deep value. Good fits (gray curves in Figure 4 with residual variance less than 1% of the variance in each mean profile) are obtained for each profile except MKE offshore of the Gulf Stream, which has a subsurface maximum that is not fit by an exponentially decaying function. To determine standard deviations of the resulting vertical scales, we add random noise with standard deviation determined by the standard error of the mean profiles and repeat the least squares fits 1,000 times. The largest resulting *e*-folding scales are 354 ± 21 m and 276 ± 11 m for MKE and EKE, respectively, in the core of the Gulf Stream. Inshore of the Gulf Stream, *e*-folding scales are 228 ± 83 and 235 ± 31 m for MKE and EKE, while offshore EKE has a vertical decay scale of 168 ± 7 m (Figure 4, boxes). For comparison, Richardson (1983c) reported an *e*-folding scale for EKE of 500 m from observations with much lower vertical resolution.

4. Summary

We have estimated the three-dimensional distributions of MKE and EKE in and near the Gulf Stream along the US East Coast using velocity observations from underwater gliders. Observations were averaged using an anisotropic and inhomogeneous Gaussian weight function that reflects both physical properties and sampling density (Figure 1). The high-MKE core along the Gulf Stream's path decays and shifts offshore with depth (Figure 3). EKE is concentrated along the Gulf Stream path with notable local maxima in the vicinity of the Charleston Bump (∼32°N) and downstream of Cape Hatteras where the current meanders. Profiles of MKE and EKE generally decay exponentially away from the surface, suggesting the possibility of parameterizing interior kinetic energy using more readily measured surface values. Vertical decay scales of MKE and EKE are larger in the core of the Gulf Stream than on the flanks (Figure 4).

MKE and EKE estimates presented here markedly improve upon the resolution and spatial extent of prior subsurface estimates of kinetic energy in the region (e.g., Owens, 1991; Richardson, 1983c; Shay et al., 1995). As such they may serve as key metrics for numerical simulations of the ocean and of the coupled climate system to reproduce. Near-surface kinetic energy estimates from the gliders are well suited for comparison to estimates of MKE and EKE from forthcoming higher resolution altimetry missions (e.g., SWOT; Morrow et al., 2019) that promise to capture fine-scale features that are not resolved by current-generation altimetry. To facilitate such intercomparisons and as encouraged by Cole et al. (2020), the MKE and EKE estimates described here are being made publicly available as described below. MKE and EKE estimates will be updated as additional glider observations are collected, reducing errors resulting from the sparseness of the glider sampling in some areas and potentially allowing for examination of seasonal-to-interannual variability in Gulf Stream kinetic energy.

Data Availability Statement

Spray glider observations used here are available from http://spraydata.ucsd.edu (Todd & Owens, 2016; Todd, 2020b). Estimates of mean velocity and kinetic energy developed here are available from http://spraydata.ucsd.edu (Todd, 2021) and will be updated periodically as new observations are obtained. Satellite altimetry data used herein were obtained from the EU CMEMS (delayed mode data from product SEALEAVEL_GLO_PHY_L4_REP_ OBSERVATIONS_008_047; near-real time data from product SEALEVEL_GLO_PHY_L4_NRT_ OBSERVATIONS_008_046). Colormaps are from Thyng et al. (2016) and from http://www.ColorBrewer.org by Cynthia A. Brewer, Pennsylvania State University.

Acknowledgments

Many people have been critical to the ongoing success of the Spray glider missions, including Patrick Deane, Joleen Heiderich, Kyle Kausch, Raymond Graham, Larry George, Ben Hodges, and Breck Owens at WHOI and Jeff Sherman, Dan Rudnick, Ben Reineman, Guilherme Castelão, and Evan Randall-Goodwin of the Instrument Development Group at the Scripps Institution of Oceanography. The Physical Oceanography Division at NOAA's Atlantic Oceanographic and Meteorological Laboratory (AOML), the University of Miami's Rosenstiel School of Marine and Atmospheric Science (RSMAS), the East Carolina University Coastal Studies Institute, and North Carolina State University's Center for Marine Sciences and Technology (CMAST) provided laboratory space for glider operations. Glider observations and analyses have been generously supported by the National Science Foundation (OCE-0220769, OCE-1558521, OCE-1633911, OCE-1923362), NOAA's Global Ocean Monitoring and Observing Program (NA14OAR4320158, NA19OAR4320074), the Office of Naval Research (N000141713040), Eastman Chemical Corporation, WHOI's Oceans and Climate Change Institute, and the W. Van Alan Clark, Jr. Chair for Excellence in Oceanography at WHOI (awarded to Breck Owens).

References

Andres, M., Donohue, K. A., & Toole, J. M. (2020). The Gulf Stream's path and time-averaged velocity structure and transport at 68.5°W and 70.3°W. *Deep-Sea Research I*, *156*, 103179. https://doi.org/10.1016/j.dsr.2019.103179

Bane, J. M., Jr, & Dewar, W. K. (1988). Gulf Stream bimodality and variability downstream of the Charleston Bump. *Journal of Geophysical Research*, *93*(C6), 6695–6710. https://doi.org/10.1029/JC093iC06p06695

Chelton, D. B., Schlax, M. G., & Samelson, R. M. (2011). Global observations of nonlinear mesoscale eddies. *Progress in Oceanography*, *91*, 167–216. https://doi.org/10.1016/j.pocean.2011.01.002

Chelton, D. B., Schlax, M. G., Samelson, R. M., Farrar, J. T., Molemaker, M. J., McWilliams, J. C., et al. (2019). Prospects for future satellite estimation of small-scale variability of ocean surface velocity and vorticity. *Progress in Oceanography*, *173*, 256–350. https://doi.org/10.1016/j.pocean.2018.10.012

Cole, S. T., Drushka, K., & Abernathey, R. (2020). Toward an observational synthesis of eddy energy in the global ocean. *US CLIVAR Variations*, *18*(1), 37–41. https://doi.org/10.5065/g8w0-fy32

Dewar, W. K., & Bane, J. M., Jr (1985). Subsurface energetics of the Gulf Stream near the Charleston Bump. *Journal of Physical Oceanography*, *15*(12), 1771–1789. https://doi.org/10.1175/1520-0485(1985)015<1771:SEOTGS>2.0.CO;2

Ferrari, R., & Wunsch, C. (2009). Ocean circulation kinetic energy: Reservoirs, sources, and sinks. *Annual Review of Fluid Mechanics*, *41*, 253–282. https://doi.org/10.1146/annurev.fluid.40.111406.102139

Gula, J., Molemaker, M. J., & McWilliams, J. C. (2015). Gulf Stream dynamics along the southeastern U.S. seaboard. *Journal of Physical Oceanography*, *45*, 690–715. https://doi.org/10.1175/JPO-D-14-0154.1

Gula, J., Molemaker, M. J., & McWilliams, J. C. (2016). Topographic generation of submesoscale centrifugal instability and energy dissipation. *Nature Communications*, *7*, 12811. https://doi.org/10.1038/ncomms12811

Halkin, D. T., & Rossby, H. T. (1985). The structure and transport of the Gulf Stream at 73°W. *Journal of Physical Oceanography*, *15*, 1439–1452. https://doi.org/10.1175/1520-0485(1985)015<1439:TSATOT>2.0.CO;2

Heiderich, J., & Todd, R. E. (2020). Along-stream evolution of Gulf Stream volume transport. *Journal of Physical Oceanography*, *50*(8), 2251–2270. https://doi.org/10.1175/JPO-D-19-0303.1

Johns, W. E., Shay, T. J., Bane, J. M., & Watts, D. R. (1995). Gulf Stream structure, transport, and recirculation near 68°W. *Journal of Geophysical Research*, *100*(C1), 817–838. https://doi.org/10.1029/94JC02497

Kang, D., & Curchitser, E. N. (2015). Energetics of eddy-mean flow interactions in the Gulf Stream region. *Journal of Physical Oceanography*, *45*(4), 1103–1120. https://doi.org/10.1175/JPO-D-14-0200.1

Kelly, K. A., & Gille, S. T. (1990). Gulf Stream surface transport and statistics at 69°W from the Geosat altimeter. *Journal of Geophysical Research*, *95*(C3), 3149–3161. https://doi.org/10.1029/JC095iC03p03149

Legeckis, R. V. (1979). Satellite observations of the influence of bottom topography on the seaward deflection of the Gulf Stream off Charleston, South Carolina. *Journal of Physical Oceanography*, *9*, 483–497. https://doi.org/10.1175/1520-0485(1979)009<0483:SOOTIO>2.0.CO;2

Morrow, R., Fu, L.-L., Ardhuin, F., Benkiran, M., Chapron, B., Cosme, E., et al. (2019). Global observations of fine-scale ocean surface topography with the Surface Water and Ocean Topography (SWOT) mission. *Frontiers in Marine Science*, *6*, 232. https://doi.org/10.3389/fmars.2019.00232

Owens, W. B. (1991). A statistical description of the mean circulation and eddy variability in the northwestern Atlantic using SOFAR floats. *Progress in Oceanography*, *28*, 257–303. https://doi.org/10.1016/0079-6611(91)90010-J

Richardson, P. L. (1983a). Eddy kinetic energy in the North Atlantic from surface drifters. *Journal of Geophysical Research*, *88*(C7), 4355–4367. https://doi.org/10.1029/JC088iC07p04355

Richardson, P. L. (1983b). Gulf Stream Rings. In A. R. Robinson (Ed.), *Eddies in marine science* (pp. 19–45). Berlin: Springer. https://doi.org/10.1007/978-3-642-69003-7_2

Richardson, P. L. (1983c). A vertical section of eddy kinetic energy through the Gulf Stream system. *Journal of Geophysical Research*, *88*(C4), 2705–2709. https://doi.org/10.1029/JC088iC04p02705

Ridgway, K. R., Dunn, J. R., & Wilkin, J. L. (2002). Ocean interpolation by four-dimensional weighted least squares—Application to the waters around Australasia. *Journal of Atmospheric and Oceanic Technology*, *19*, 1357–1375. https://doi.org/10.1175/1520-0426(2002)019<1357:OIBFDW>2.0.CO;2

Roemmich, D., & Gilson, J. (2009). The 2004–2008 mean and annual cycle of temperature, salinity, and steric height in the global ocean from the Argo Program. *Progress in Oceanography*, *82*(2), 81–100. https://doi.org/10.1016/j.pocean.2009.03.004

Rossby, T. (1987). On the energetics of the Gulf Stream at 73W. *Journal of Marine Research*, *45*, 59–82. https://doi.org/10.1357/002224087788400918

Rossby, T., & Gottlieb, E. (1998). The Oleander Project: Monitoring the variability of the Gulf Stream and adjacent waters between New Jersey and Bermuda. *Bulletin of the American Meteorological Society*, *79*(1), 5–18. https://doi.org/10.1175/1520-0477(1998)079<0005:TOPMTV>2.0.CO;2

Rossby, T., & Zhang, H.-M. (2001). The near-surface velocity and potential vorticity structure of the Gulf Stream. *Journal of Marine Research*, *59*, 949–975. https://doi.org/10.1357/00222400160497724

Roullet, G., Capet, X., & Maze, G. (2014). Global interior eddy available potential energy diagnosed from Argo floats. *Geophysical Research Letters*, *41*, 1651–1656. https://doi.org/10.1002/2013GL059004

Rudnick, D. L., & Cole, S. T. (2011). On sampling the ocean using underwater gliders. *Journal of Geophysical Research*, *116*, C08010. https://doi.org/10.1029/2010JC006849

Rudnick, D. L., Davis, R. E., & Sherman, J. T. (2016). Spray underwater glider operations. *Journal of Atmospheric and Oceanic Technology*, *33*(6), 1113–1122. https://doi.org/10.1175/JTECH-D-15-0252.1

Rudnick, D. L., Zaba, K. D., Todd, R. E., & Davis, R. E. (2017). A climatology of the California Current System from a network of underwater gliders. *Progress in Oceanography*, *154*, 64–106. https://doi.org/10.1016/j.pocean.2017.03.002

Rypina, I. I., Kamenkovich, I., Berloff, P., & Pratt, L. J. (2012). Eddy-induced particle dispersion in the near-surface North Atlantic. *Journal of Physical Oceanography*, *42*, 2206–2228. https://doi.org/10.1175/JPO-D-11-0191.1

Schmitz, W. J., Jr (1976). Eddy kinetic energy in the deep western North Atlantic. *Journal of Geophysical Research*, *81*(27), 4981–4982. https://doi.org/10.1029/JC081i027p04981

Schmitz, W. J., Jr (1978). Observations of the vertical distribution of low frequency kinetic energy in the Western North Atlantic. *Journal of Marine Research*, *36*(2), 295–310. https://doi.org/10.1575/1912/10629

Schmitz, W. J., Jr (1984). Abyssal eddy kinetic energy in the North Atlantic. *Journal of Marine Research*, *42*, 509–536. https://doi.org/10.1357/002224084788505933

Shay, T. J., Bane, J. M., Watts, D. R., & Tracey, K. L. (1995). Gulf Stream flow field and events near 68°W. *Journal of Geophysical Research*, *100*(C11), 22565–22589. https://doi.org/10.1029/95JC02685

Sherman, J., Davis, R. E., Owens, W. B., & Valdes, J. (2001). The autonomous underwater glider "Spray". *IEEE Journal of Oceanic Engineering*, *26*(4), 437–446. https://doi.org/10.1109/48.972076

Stammer, D. (1997). Global characteristics of ocean variability estimated from regional TOPEX/POSEIDON altimeter measurements. *Journal of Physical Oceanography*, *27*, 1743–1769. https://doi.org/10.1175/1520-0485(1997)027<1743:GCOOVE>2.0.CO;2

Szuts, Z. B., Bower, A. S., Donohue, K. A., Girton, J. B., Hummon, J. M., Katsumata, K., et al. (2019). The scientific and societal uses of global measurements of subsurface velocity. *Frontiers in Marine Science*, *6*, 358. https://doi.org/10.3389/fmars.2019.00358

Thyng, K. M., Greene, C. A., Hetland, R. D., Zimmerle, H. M., & DiMarco, S. F. (2016). True colors of oceanography: Guidelines for effective and accurate colormap selection. *Oceanography*, *29*(3), 9–13. https://doi.org/10.5670/oceanog.2016.66

Todd, R. E. (2017). High-frequency internal waves and thick bottom mixed layers observed by gliders in the Gulf Stream. *Geophysical Research Letters*, *44*, 6316–6325. https://doi.org/10.1002/2017GL072580

Todd, R. E. (2020a). Export of Middle Atlantic Bight shelf waters near Cape Hatteras from two years of underwater glider observations. *Journal of Geophysical Research*, *125*, e2019JC016006. https://doi.org/10.1029/2019JC016006

Todd, R. E. (2020b). *Spray glider observations in support of PEACH [Data set]*. Scripps Institution of Oceanography, Instrument Development Group. https://doi.org/10.21238/S8SPRAY0880

Todd, R. E. (2021). *Gulf Stream mean and eddy kinetic energy from Spray underwater glider measurements [Data set]*. Scripps Institution of Oceanography, Instrument Development Group. https://doi.org/10.21238/S8SPRAY2675A

Todd, R. E., & Owens, W. B. (2016). *Gliders in the Gulf stream [Data set]*. Scripps Institution of Oceanography, Instrument Development Group. https://doi.org/10.21238/S8SPRAY2675

Todd, R. E., Owens, W. B., & Rudnick, D. L. (2016). Potential vorticity structure in the North Atlantic western boundary current from underwater glider observations. *Journal of Physical Oceanography*, *46*(1), 327–348. https://doi.org/10.1175/JPO-D-15-0112.1

Todd, R. E., Rudnick, D. L., Sherman, J. T., Owens, W. B., & George, L. (2017). Absolute velocity estimates from autonomous underwater gliders equipped with Doppler current profilers. *Journal of Atmospheric and Oceanic Technology*, *34*(2), 309–333. https://doi.org/10.1175/JTECH-D-16-0156.1

Watts, D. R., & Johns, W. E. (1982). Gulf Stream meanders: Observations on propagation and growth. *Journal of Geophysical Research*, *87*(C12), 9467–9476. https://doi.org/10.1029/JC087iC12p09467

Wyrtki, K., Magaard, L., & Hager, J. (1976). Eddy energy in the oceans. *Journal of Geophysical Research*, *81*(15), 2641–2646. https://doi.org/10.1029/JC081i015p02641

Yu, X., Ponte, A. L., Elipot, S., Menemenlis, D., Zaron, E. D., & Abernathey, R. (2019). Surface kinetic energy distributions in the global oceans from a high-resolution numerical model and surface drifter observations. *Geophysical Research Letters*, *46*, 9757–9766. https://doi.org/10.1029/2019GL083074

Zeng, X., & He, R. (2016). Gulf Stream variability and a triggering mechanism of its large meander in the South Atlantic Bight. *Journal of Geophysical Research*, *121*, 8021–8038. https://doi.org/10.1002/2016JC012077

Zhai, X., Johnson, H. L., & Marshal, D. P. (2010). Significant sink of ocean-eddy energy near western boundaries. *Nature Geoscience*, *3*, 608–612. https://doi.org/10.1038/ngeo943